IOPscience iopscience.iop.org

Home Search Collections Journals About Contact us My IOPscience

Transport mechanism of nanocrystalline-silicon film tunnelling diodes

This article has been downloaded from IOPscience. Please scroll down to see the full text article.

1999 J. Phys.: Condens. Matter 11 8495

(http://iopscience.iop.org/0953-8984/11/43/312)

View the table of contents for this issue, or go to the journal homepage for more

Download details:
IP Address: 171.66.16.220
The article was downloaded on 15/05/2010 at 17:41

Please note that terms and conditions apply.

J. Phys.: Condens. Matter **11** (1999) 8495–8504. Printed in the UK PII: S0953-8984(99)04051-5

Transport mechanism of nanocrystalline-silicon film tunnelling diodes

G Y Xu†‡‖, M Liu‡, X S Wu§, Y L He‡§ and T M Wang†‡

† Department of Material Science, Lanzhou University, Lanzhou 730000, People's Republic of China

‡ Material Physics and Chemistry Research Center of BUAA, Beijing 100083, People's Republic of China

§ Department of Physics, Nanjing University, Nanjing 210008, People's Republic of China

E-mail: xugy@beta.ihepa.ac.cn

Received 6 May 1999

Abstract. Based on the research into the conduction mechanism of the hydrogenated nanocrystalline silicon (nc-Si:H) films, we have fabricated nanocrystalline-silicon film tunnelling diodes. The structure of the diode is Al/c-Si/nc-Si:H/Al, in which the nc-Si:H thin film is the active layer. A characteristic of local ordered structures was detected in the nc-Si:H film, which indicated that both ordered micro-zones and disordered regions existed in the film. In some diodes quantum staircases and quantum oscillation phenomena were observed in the I–V, σ–V and C–V curves at liquid nitrogen temperatures or below (<100 K). On the basis of energy level calculation, we consider that the current through the diode comes from two parts: in the ordered micro-zones of the active layer electrons transport via resonant tunnelling, while in the disordered regions resonant tunnelling will be smeared and the tunnelling current increases continually with increasing bias.

Nomenclature

nc-Si:H	hydrogenated nanocrystalline silicon film
ΔE	active energy of hydrogenated nanocrystalline silicon film
E_c	conduction band edge of hydrogenated nanocrystalline silicon film
$\Delta\Theta$	angular deviation from the Bragg angle in the double-crystal x-ray diffraction pattern
$\Delta\Theta_{\max I}$	angular distance between the mth order peak and symmetrical (111) Si reflection
λ	wavelength of Cu Kα_1, $\lambda = 0.154$ nm
L	arrangement period of the silicon grains in the ordered micro-zone
h	reduced Planck constant
$V(r)$	potential function
Ψ	wave function
V_0	height of the barrier, $V_0 = 0.5$ eV
a	radius of silicon grain
E_{n0}	energy level of the nth quantum state when all levels are empty
E_n	energy level of the nth quantum state when occupied by n electrons

‖ Corresponding author. Present address: The Amorphous Physics Research Laboratory, Beijing University of Aeronautics and Astronautics, Beijing 100083, People's Republic of China.

0953-8984/99/438495+10$30.00 © 1999 IOP Publishing Ltd

E_{FM}	Fermi level of the Al gate
E_{FS}	Fermi level of c-Si substrate
$-V_A$	the negative bias
$\Delta\omega$	the peak shift in Raman spectra for the nanocrystalline as compared with that of c-Si (520.0 cm^{-1})
B	a constant of 2.0 cm^{-1} nm^2

1. Introduction

Research on low-dimensional semiconductor systems has led to the development of quantum dot (QD) arrays on crystalline Si and GaAs wafers using photolithography technology [1, 2]. Coulomb blockade effects, quantum oscillation, negative differential conductance etc have been observed in the liquid helium temperature range. Some of them have become the basis for the development of quantum functional devices [3, 4]. However, the low operational temperature makes these artificial QD systems of little practical value. On the other hand, another kind of low-dimensional silicon systems, such as porous silicon and nc-Si/a-SiO_2 (nano-silicon particles embedded in amorphous silica) have caused considerable interest [5–8]. A common feature of these materials is that the size distribution of the nc grains is normally random. Therefore, we call them natural quantum confinement (NQC) systems. Many novel characteristics have been found in these NQC systems, for example visible light emission from porous silicon and nc-Si/a-SiO_2 [5, 6]. Especially, resonant tunnelling was observed close to room temperature in the nc-Si/a-SiO_2 system [7, 8]. These works received much attention for they proposed that in natural quantum confinement systems, if the size distribution of the grains can be limited in a narrow range, quantum confinement effects such as Coulomb oscillation and resonant tunnelling can be realized at higher temperature than in AQCs.

Also of interest, in the same context, are nc-Si:H films. A typical nc-Si:H film is composed approximately of 50% nanocrystalline silicon with mean grain size 3–6 nm and 50% amorphous Si in the interface regions among the grains. The thickness of the interface is around 2–4 atomic spacings. Based on the microstructure characteristics of the nc-Si:H films, the dependence of film conductivity on mean grain size and crystalline percentage, the temperature characteristic of the film conductivity, we have concluded that the nanoscale silicon grains in nc-Si:H films possess quantum dot characteristics both in their microstructures and electrical properties. A heterojunction quantum dot (HQD) model was proposed to explain the transport mechanism of nc-Si:H films [9]. In the HQD model the main physical concepts are that the nanocrystalline grains and their interface regions have very different band gaps and band structures. As a result, they form heterojunction structures in which the amorphous interface regions act as barriers and the silicon grains act as potential wells. Moreover, in the presence of an external field, activated electrons transport ballistically in silicon grains and pass through the interface barriers via single electron tunnelling. A complete conductivity formula for nc-Si:H films was proposed from the HQD model. The values of activation energy ΔE and conduction band edge E_c calculated theoretically from the formula are in good agreement with the experimental data [10].

On this basis, we developed tunnelling diodes from the nc-Si:H thin film. Quantum staircases, and quantum oscillation phenomena, were observed in the I–V, σ–V, and C–V curves at liquid nitrogen temperatures or below. These characteristics are closely related to the microstructure of the nc-Si:H film. Combining the quantum confinement and Coulomb blockade effects we calculated the discrete levels of an individual silicon grain. Furthermore, the deviation of the grains was also considered. On this basis a qualitative explanation for the experimental phenomena was achieved. This work not only confirms the quantum transport

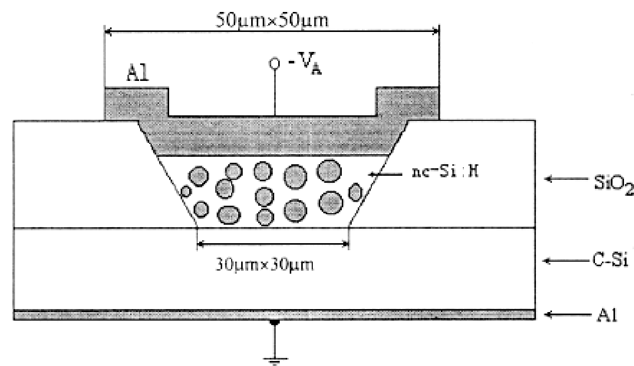

Figure 1. The cross-section of the nc-Si:H tunnelling diode.

mechanism of the nc-Si:H film, but also proposes application of the nc-Si:H film in the field of semiconductor quantum functional devices.

2. Experiment

The cross-sectional configuration of the tunnelling diode is shown in figure 1. First, an SiO_2 layer around 200 nm in thickness was prepared by thermal oxidation of an n-type c-Si(100) wafer at 1020 °C (the resistivity of the wafer was about 1–2 Ω cm). The SiO_2 layer was etched and patterned by photolithography to make an array of square holes (30 μm × 30 μm). After appropriate treatment, a fresh nc-Si:H layer around 20 nm in thickness was deposited on the array configuration. The nc-Si:H layers were prepared in a plasma-enhanced chemical vapour deposition (PECVD) system by rf (13.56 MHz) and dc bias stimulation. A strongly hydrogen diluted silane, i.e. SiH_4 diluted to 1% in H_2 was used as the reactant gas source to produce the nanostructured samples at a substrate temperature T_s of 250 °C, with a power density of 0.6 W cm^{-2}. A negative −200 V dc bias was applied to the substrate. The total pressure of reactive gases in the deposition process was 1.0 Torr. The details of the experimental parameters were described elsewhere [11]. The outer layer of the nc-Si:H films in the square holes was removed by etching and photolithography, leaving only very thin nc-Si:H layers in the hole bottoms. Finally, the Al gates (50 μm × 50 μm) and Al substrate contacts (after etching away SiO_2 on the wafer backside) were deposited by vacuum evaporation. This gave the Al/c-Si/nc-Si:H/Al tunnelling diode structure.

The interface between the nc-Si:H layer and c-Si substrate was examined by high resolution transmission microscopy (HREM). Microstructure of the nc-Si:H films were measured by means of Raman scatter and double-crystal x-ray diffraction (Cu Kα_1 radiation). The σ–V, I–V, and C–V characteristics of the tunnelling diodes were measured at liquid nitrogen temperatures or below (<100 K).

3. Results and discussion

3.1. The microstructure of nc-Si:H layers

In order to explain the transport mechanism of the tunnelling diodes, it is very necessary to study deeply the microstructure of the nc-Si:H layer. The HREM picture, shown in figure 2, confirms that the thin nc-Si:H layer deposited on the c-Si substrate was really nanocrystalline

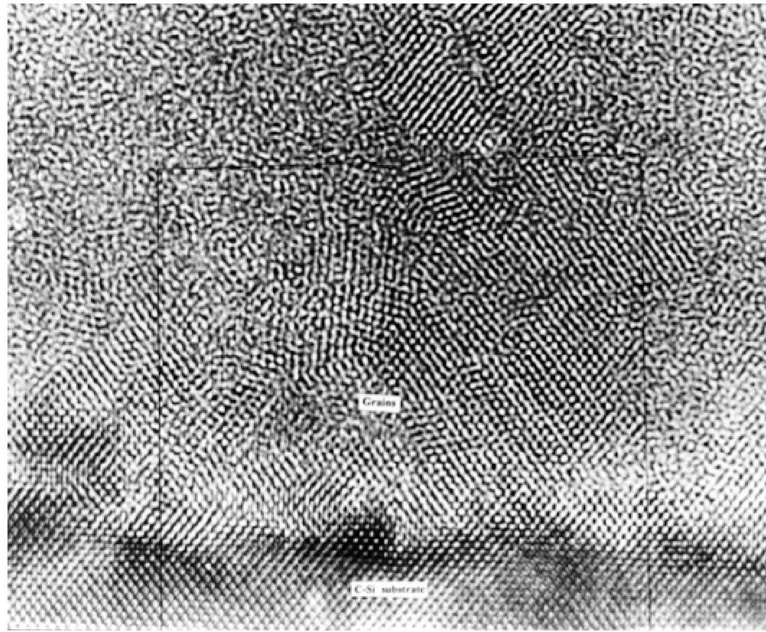

Figure 2. HREM photo of thin nc-Si:H film on c-Si substrate.

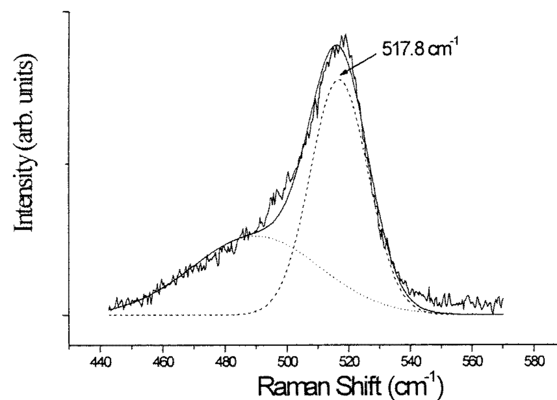

Figure 3. The Raman spectra of the TO-like mode for the nc-Si:H film which can be decomposed into an amorphous component (dotted line) and crystalline ones (dashed line). The solid curve is a sum of these two contributions.

without an amorphous buffer layer. Figure 3 shows a typical Raman spectrum of a TO-like mode for the nc-Si:H layer which contains the characteristic peak of the amorphous component at 480 cm^{-1} and crystalline ones at 517.8 cm^{-1} respectively. We calculated the average size d of the nanocrystallites according to the formula [12]:

$$d = 2\pi(B/\Delta\omega)^{1/2} \tag{1}$$

where B is a constant of 2.0 cm^{-1} nm^2, $\Delta\omega$ is the peak shift for the nanocrystalline as compared with that of the c-Si (520.0 cm^{-1}). From figure 3 the average grain size is calculated to be 6 nm. According to the thickness of the active layer, the nc-Si:H layer most likely consists of two to three grains connected in the depth direction.

Figure 4 is the double-crystal x-ray diffraction spectrum for the surface of the nc-Si:H layer. The symmetrical satellite peaks around the (111) Si reflection indicate local periodic structure in the film [13]. That is, there are some ordered micro-zones in the film where the silicon grains keep approximately uniform in size and spacing. This periodical arrangement of the silicon grains, like artificially fabricated quantum dots, causes the interference maxima around the symmetrical (111) Si reflection up to the fourth order. Using equation (8) in [13],

$$\Delta\Theta_{\max I} = \arcsin(m\lambda/L) \tag{2}$$

we calculate from the angular distance between the +1 and −1 peaks ($\sim 13°$) the arrangement period $L = 6.3 \pm 0.5$ nm. The arrangement period L is approximately the sum of the silicon grain diameter and the thickness of the interface layer. So, in the film there are some ordered micro-zones where the grains are approximately uniform in size and spacing, coexisting with disordered regions where grains distribute randomly. We consider that this structural characteristic plays a dominant role in the electrical properties of the tunnelling diodes.

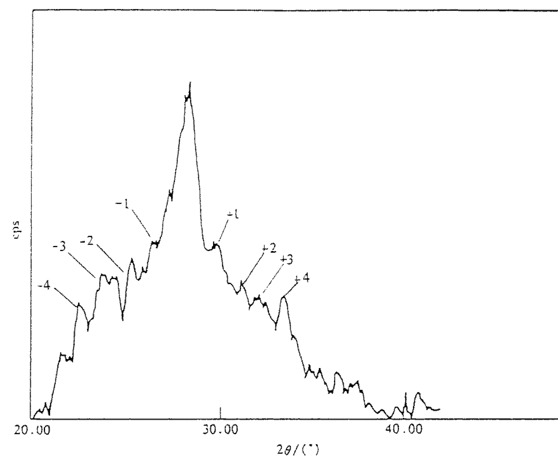

Figure 4. The double-crystal x-ray diffraction spectrum (Cu Kα_1 radiation) of the surface of the nc-Si:H films.

3.2. Transport mechanism of the tunnelling diodes

The I–V characteristic of the diodes was measured at 77 K, and typical results are shown in figure 5. For sample 1 the current increases continually with increasing bias and no current staircase is observed. But for samples 2–4 current staircases appear in the bias range of −7 V to −9 V, and the number of current staircases varies with different samples. Especially in sample 4 a clear flat current region, which is a characteristic of the Coulomb blockade structure, was observed. As further studies, the σ–V and C–V characteristics of sample 4 were measured, and the results are shown in figures 6 and 7 respectively. In figure 6 there is a conductance peak near zero volts which is caused by electron capture and emission by interface traps at the nc-Si:H/c-Si interface. A similar result was also observed in the nc-Si/SiO_2 system [14]. In the −7 V to −9 V range, where current staircases were found in the I–V curve, there are three quantum staircases in the σ–V curve. Simultaneously, figure 7 shows three oscillatory discontinuities in the same bias range in the C–V curve. These experimental phenomena tend to prove that quantum staircase and oscillatory discontinuities in the I–V, σ–V and C–V curves are caused by the activated electrons transporting through the nc-Si:H layer via

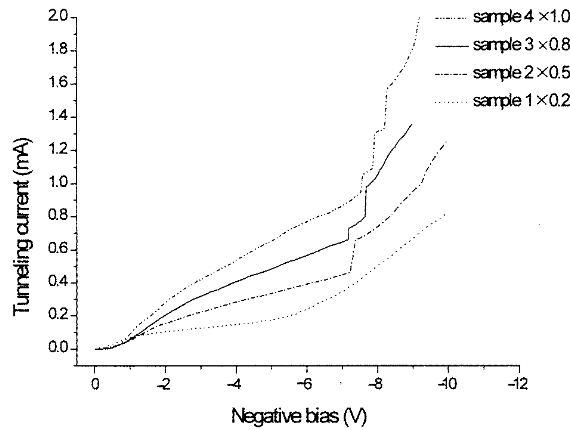

Figure 5. I–V curves of four nc-Si film tunnelling diodes measured at 77 K. To separate the curves, the tunnelling current of each sample is multiplied by a factor which is noted in the figure.

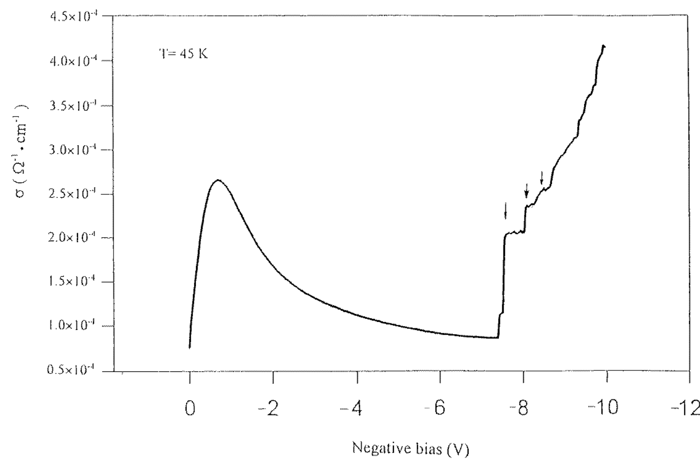

Figure 6. The σ–V characteristic curve of sample 4 at 45 K.

resonant tunnelling. We tentatively explain the transport mechanism in the tunnelling diodes as follows.

The first step to explain the electron transport mechanism is to calculate levels in an individual silicon grain. From the HQD model, the height of the barriers is about 0.5 eV [10]. For such a low barrier the infinite deep well model is no longer reliable. Therefore, a finite deep well model is used here. For a spherical silicon grain of radius a, the Schrödinger function is

$$\left[-\frac{h^2}{2m^*}\nabla^2 + V(r)\right]\Psi = E\Psi$$
$$V(r) = 0 \qquad \text{when } r < a$$
$$V(r) = V_0 \qquad \text{when } r \geqslant a \tag{3}$$

where V_0 is the height of the barrier and m^* is the effective mass of a tunnelling electron [15]. For a silicon grain whose radius $a = 3.0$ nm the resulting eigenvalues E_{n0} are shown in figure 8(a). Due to the limit of the barrier height and grain size only three levels are permitted

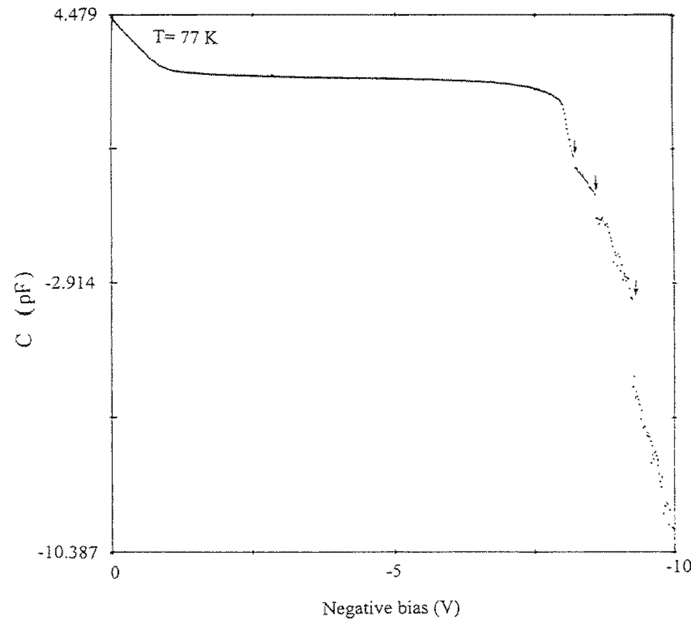

Figure 7. The C–V characteristic curve of sample 4 at 77 K.

in this case. On the other hand, the Coulomb energy (the so-called Coulomb blockade effect) makes the eigenlevels higher and further apart in energy. Considering the Coulomb energy, the eigenlevel of the nth quantum state is [14]

$$E_n = E_{n0} + n\left(\frac{e^2}{2C}\right) \tag{4}$$

where E_{n0} is the energy level of the nth quantum state when all levels are empty, E_n is the energy level of the nth quantum state occupied by n electrons and n denotes the quantum states in ascending energy. C is the capacitance of an nc-silicon grain. However, because the grains are nanoscaled and embedded in an amorphous matrix, an accurate calculation of C is difficult. Experimentally, Raphael Tsu [16] defined C in terms of an increment of the total stored energy in the grain. This universal definition of C gives values below than what can be calculated from electrostatics. Using the method mentioned above the value of C in our case is estimated to be 4 aF, yielding the Coulomb energy ($e^2/2C$) of about 20 meV. The energy levels modified by the Coulomb blockage effect are shown in Figure 8(b). Consider next the influence of grain size variation on the energy levels. For the same order of quantum state, the level in a small grain is higher in energy than that in a larger grain. Hence, levels for the same order in different grains will form a band as shown in figure 8(c), which shows the effect on the levels with a 20% variation in grain size.

With the background just given, the schematic potential landscape of the tunnelling diode (including two quantum dots, QD1 and QD2, in the depth direction) is given in figure 9, where the shaded regions represent the bands discussed above. Resonant tunnelling occurs only when the Fermi level of the Al gate is swept through the separated bands of QD1. For some diodes, the deviation of the silicon grain size is too wide, and therefore the bands are broadened and overlapped. That is, in the whole active layer the levels of different silicon grains are semi-continuous in energy. As a result, resonant tunnelling will be smeared, as in the case of sample

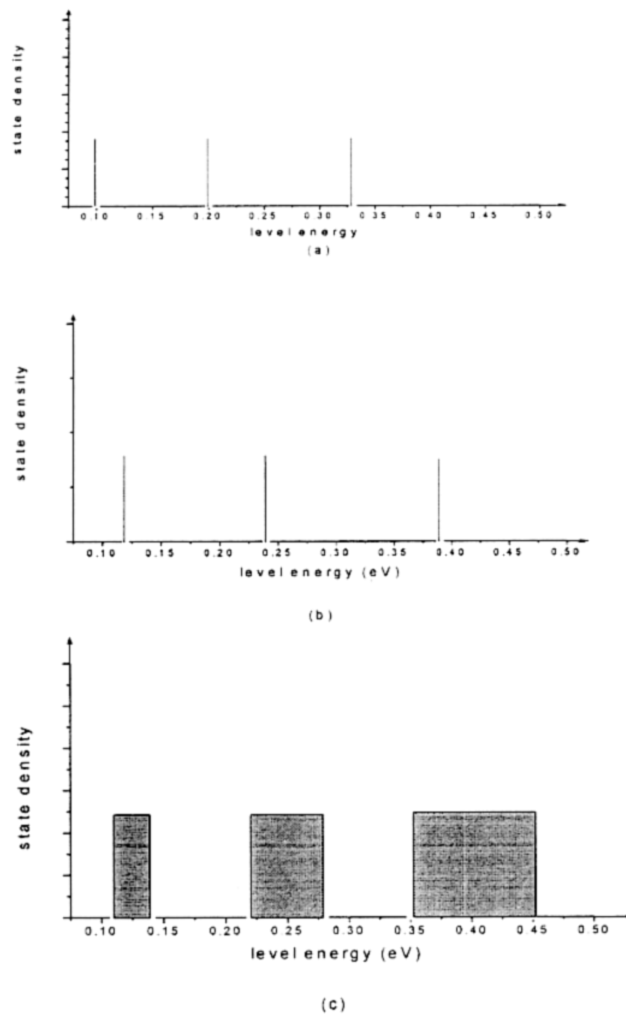

Figure 8. (a) Calculated energy levels for a sphere of radius 3 nm. (b) Density of states against energy in a silicon grain due to the Coulomb blockade effect. (c) Variation in silicon grain size is considered.

1 in figure 5. But for others where there are ordered micro-zones in nc-Si:H layers, the case will be different. In these ordered zones the grain size varies in a narrow range, and therefore the bands become narrower. Partial bands begin to separate from others. Through the separated bands resonant tunnelling occurs in the ordered zones. It will be reflected in the I–V curves, as in sample 2 and 3 in figure 5, in which partial current steps were observed. We also noted that in sample 3, between the steps the current does not keep constant but increases continually with increasing bias. This is different from the case of artificial quantum dots. This extra current may be caused by the disordered regions in the nc-Si:H layers. In these disordered regions resonant tunnelling will be smeared out and the tunnelling current increase continually with increasing bias. Tsu's group also reported similar phenomena in the nc-Si/a-SiO_2 system [14]. Only when the silicon grains are highly uniform in size can all three bands be narrow enough to separate completely from one another, and therefore all three current steps appear

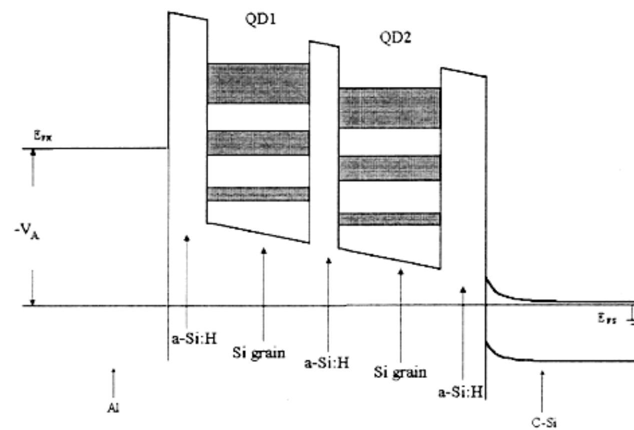

Figure 9. The schematic potential landscape of a grain array including two quantum dots. The shaded regions represent the energy bands. $E_{\rm FM}$ is the Fermi level of the Al gate and $E_{\rm FS}$ is that of c-Si. $-V_{\rm A}$ is the negative bias.

in the I–V curve. Sample 4 in figure 5 is a good example. Moreover, in sample 4 there are clear flat current regions between the quantum staircases, which is the characteristic for the Coulomb blockage effect. This also illustrates that in sample 4 the deviation of the silicon grains is very small.

Notably, the σ–V characteristic of sample 4 (figure 6) is correspondent with the I–V characteristic. It is convenient to explain the staircase in the σ–V curve by the resonant tunnelling model. When the Fermi level (E_{FM}) of the Al gate is swept through one separated band, resonant tunnelling occurs and the tunnelling current increases steeply. This causes a jump of conductivity in the σ–V curve. Before E_{FM} is swept through the next band the tunnelling current increases very slowly, and therefore a flat conductivity region forms in the σ–V curve. This characteristic is similar to that of figure 4(a) in [14]. We also found that in the C–V curve of sample 4 there are three quantum oscillatory discontinuities in the corresponding bias range. All of these experimental phenomena directly prove that resonant tunnelling is an important transport mechanism in the Al/c-Si/nc-Si:H/Al tunnelling diodes.

4. Conclusion

In conclusion, we have fabricated Al/c-Si/nc-Si:H/Al tunnelling diodes by using the nc-Si:H thin film as active layer. The microstructure and electrical properties of the tunnelling diodes were systematically studied. The active layer is exactly composed by nanoscale silicon grains and an amorphous Si:H interface. A characteristic of local ordered structures was detected in the nc-Si:H film, which indicates that both ordered micro-zones and disordered regions exist in the film. Quantum confinement effects were observed at liquid nitrogen temperature or below. The transport mechanism of the tunnelling diodes can be summarized as:

(1) In the ordered micro-zones, electrons transport by resonant tunnelling.
(2) In the disordered regions, resonant tunnelling will be smeared and the tunnelling current increases continually with increasing bias.

The total current following through the diode is the sum of these two parts. This model is in consistence with the heterojunction quantum dot (HQD) model for nc-Si:H films, and

qualitatively explains the I–V, σ–V and C–V characteristics of the nanocrystalline-silicon tunnelling diodes.

In this work, quantum confinement was observed in a structure prepared by film growth rather than photolithography with the advantages of greater fabrication simplicity and higher operational temperature. This confirms Tsu's view that quantum confinement can be realized not only in artificial quantum dots (AQD) systems, but also in natural quantum dots (NQDs). The observations reported in nc-Si:H tunnelling diodes open the way for much wider applications of quantum confinement phenomena.

Acknowledgments

The electrical measurements and Raman scattering measurement were accomplished in the Beijing Semiconductor Institution, Academia Sinica. The HREM picture was made by Dr D P Yu in Beijing Electron Microscopy Laboratory, Academia Sinica. It is our pleasure to acknowledge them for their contribution. The work is supported by the National Science Foundation of China.

References

[1] Van der Vaar N C and Molenkamp L W 1995 *Phys. Rev. Lett.* **74** 4702
[2] Shingo Kasumoto *et al* 1992 *Japan. J. Appl. Phys.* **31** 759
[3] Tsu R and Esaki L 1993 *Appl. Phys. Lett.* **22** 562
[4] Reed M A *et al* 1988 *Phys. Rev. Lett.* **60** 535
[5] Canham L T 1990 *Appl. Phys. Lett.* **57** 1046
[6] Lowe-Webb R R *et al* 1998 *J. Appl. Phys.* **83** 2815
[7] Nicollian E H and Tsu R 1993 *J. Appl. Phys.* **74** 4020
[8] Chou S Y and Gorden A E 1992 *Appl. Phys. Lett.* **60** 1827
[9] He Y E *et al* 1999 *Phys. Rev.* B **59** 15 352
[10] Hu G Y *et al* 1995 *J. Appl. Phys.* **78** 3845
[11] He Y L *et al* 1994 *J. Appl. Phys.* **72** 797
[12] Cardona M and Guntherodt 1982 *Light Scattering in Solids II* (Berlin: Springer) p 80
[13] Tapfer L and Grambow P 1990 *Appl. Phys.* A **50** 3
[14] Ye Qiu-Yi *et al* 1991 *Phys. Rev.* B **44** 1806
[15] Yoshida T *et al* 1995 *Japan. J. Appl. Phys.* **34** L903
[16] Tsu R 1993 *Physica* B **189** 235